

THE INTRINSIC HIGH METALLICITY OF CSNRs

A. Rodríguez-González, G. Tenorio-Tagle and S. Silich

Instituto Nacional de Astrofísica Óptica y Electrónica, Puebla, México

RESUMEN

Aquí presentamos soluciones semianalíticas de la hidrodinámica de remanentes de supernova compactos (cSNRs) y su evolución química. Discutimos dos modelos de explosiones de supernova de $15 M_{\odot}$ y $25 M_{\odot}$, envueltas en un medio denso ($n_0 \sim 10^7 \text{ cm}^{-3}$). Demostramos que después de algunos años de evolución, la difusión produce una distribución homogénea de los productos de la SN dentro de los delgados cascarones fríos formados después del enfriamiento del material barrido. Encontramos metalicidades en un intervalo de $5.5 \leq Z_O/Z_{\odot} \leq 6.0$ para $M_{SN} = 25 M_{\odot}$ y $1.0 \leq Z_O/Z_{\odot} \leq 1.5$ para $M_{SN} = 15 M_{\odot}$, y especulamos que estas metalicidades están relacionadas con las abundancias observadas en QSOs (Ferland et al. 1996; Hamann & Ferland 1999).

ABSTRACT

Here we present semi-analytical solutions of the hydrodynamics of compact supernova remnants (cSNRs) and their chemical evolution. Two models of $15 M_{\odot}$ and $25 M_{\odot}$ supernova explosions evolving in a high density medium ($n_0 \sim 10^7 \text{ cm}^{-3}$) are thoroughly discussed. We demonstrate, that after a few years of evolution, diffusion leads to an homogeneous distribution of the SN products inside the cold, thin shell formed after cooling of the swept-up matter sets in. We find metallicity values within a range $5.5 \leq Z_O/Z_{\odot} \leq 6.0$ for $M_{SN} = 25 M_{\odot}$ and $1.0 \leq Z_O/Z_{\odot} \leq 1.5$ for $M_{SN} = 15 M_{\odot}$, and speculate whether these metallicities could be related to the observed QSOs super solar elemental abundances (Ferland et al. 1996; Hamann & Ferland 1999).

Key Words: **SUPERNOVA REMNANTS — QUASARS : GENERAL**

1. INTRODUCTION

The discovery of the high-redshift quasars (QSO) implies that massive star formation occurs very early in galaxy evolution. Spectra of high redshifted QSOs ($z > 4$) present broad line emission (Hamann & Ferland, 1993) which is similar to that seen in active galactic nuclei (AGNs). The metallicities of the associated fast moving gas derived from the spectral analysis are surprisingly high for so young objects and fall into the range $Z_{\odot} \leq Z \leq 9Z_{\odot}$ (Hamann & Ferland 1999).

These results have a great interest because provide information about an early history of star formation in galaxies. If high metallicity is related to a short episode of star formation, it has to occur at early (few Gyr) stages of galaxies evolution and suggests a fast mixing of ejected metals with a bulk of primordial low metallicity gas (Hamann & Ferland, 1993; Ferland et al. 1996). Different modifications of this scenario have been proposed by Silk & Rees (1998) who have discussed an enhanced star formation inside an accretion disk.

The observed quasar (and AGN) spectra show a great similarity to the spectra of type II peculiar

supernova remnants (Terlevich et al. 1992) which one believes to be a compact SNR (cSNR) evolving in a very dense ($\sim 10^7 \text{ cm}^{-3}$) circumstellar environment. Therefore here we analyze an alternative scenario based on the starburst model of AGNs (Terlevich et al. 1992). For the calculations we use a semi-analytical model of the young supernova remnant evolution and thoroughly discuss the dispersal of the ejected metals into the swept-up primordial gas. We simulate cSNRs evolution from the $15 M_{\odot}$ and $25 M_{\odot}$ progenitors and show that model predicted thicknesses, densities and temperatures allow a fast mixing of the abundant ejecta with the swept-up low metallicity circumstellar material. The resultant cSNR abundances fall into the observed QSOs metallicity range.

2. THE INPUT MODEL

2.1. Ejecta model

The interaction of the SN ejected matter with the surrounding medium causes a four zone structure: the inner free expanding ejecta which is bounded by a reverse shock with radius R_{RS} and velocity D_{RS} ; the shocked ejecta which is accommodated between

the reverse shock position and the contact discontinuity R_{CD} ; the shocked CSM which is separated from the ejected material by the CD and from the surrounding medium by the leading shock with radius R_{LS} and velocity D_{LS} . The outward shock sweeps-up the dense surrounding medium and enhances its temperature to $\sim 10^8$ K. The reverse shock is slower and thermalizes the SN ejecta.

The cSNR initial evolution is dependent on the surrounding gas number density and the ejecta density and velocity radial distribution. We adopt Franco et al. (1991) analytical model based on Woosley et al. (1988) calculations. It assumes that supernova ejecta obey the free expansion law with r^{-3} density and linear velocity distributions:

$$\rho_{ej}(r, t) = \begin{cases} M_{ej} r^{-3} / 4\pi \ln \left(\frac{R(t)}{R_c} \right), & r \geq R_c \\ 0 & r < R_c \end{cases} \quad (1)$$

$$V_{ej}(r, t) = \begin{cases} \frac{r - R_c}{R(t) - R_c} V_m, & r \geq R_c \\ 0 & r < R_c \end{cases} \quad (2)$$

where $R(t) = R_m + V_m t$, R_m is the initial radius and V_m is the maximum ejecta velocity, R_c is the inner radius of the ejecta. The total mass of ejecta and masses of the ejected oxygen and iron have been taken from Woosley (1978) model. The initial model parameters are summarized in the Table 1.

TABLE 1

INITIAL CONDITIONS		
	15 M_\odot	25 M_\odot
Initial energy [erg]	1×10^{51}	1×10^{51}
Ejecta mass [M_\odot]	13.44	23.61
Maximum velocity [$km\ s^{-1}$]	6000	5000
R_c [cm]	6.45×10^{15}	3.24×10^{15}
R_m [cm]	3.82×10^{16}	4.10×10^{16}
Ejecta mass of oxygen [M_\odot]	0.42	3.0
Ejecta mass of iron [M_\odot]	0.06	0.08

2.2. The dispersal of metals

There are essentially two irreversible mass transport mechanisms leading to the dispersal of the heavy elements released during the supernova explosions throughout the ISM. They are diffusion and turbulent mixing (Roy & Kunth, 1995; Tenorio-Tagle, 1996; Oey 2003). The determination of the

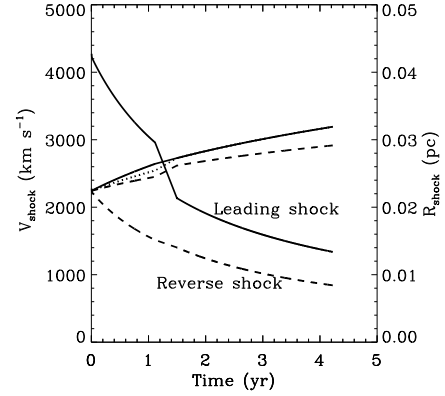


Fig. 1. Radius and velocity evolution of the shocks.

appropriate turbulent parameters so far is speculative. Therefore here we focus on the diffusion of the supernova ejected metals and their mixing with the swept-up CSM.

We assume that the ejecta represents a homogeneous mixture of the progenitor outer hydrogen envelope with the synthesized heavy elements. At the contact discontinuity this high metallicity gas is mixed with the low metallicity circumstellar material. The characteristic diffusion time over a length L is $t_D = L^2/D$, where D is the diffusion coefficient. When the dynamical time t exceeds the characteristic diffusion time t_D , the metallicity of the mixture approach the value

$$Z_A(t)/Z_\odot = \frac{M_{A\ ej}(t)/Z_{A\ \odot} + Z_{ISM} M_{ISM}(t)}{M_{ISM}(t) + \chi M_{ej}(t)} \quad (3)$$

where $M_{CSM}(t)$ and $\chi M_{ej}(t)$ are masses of the swept-up CSM and the ejecta, respectively, and $M_{A\ ej}(t)$ is the mass of the element A that has been accumulated within a given gaseous segment.

3. THE RESULTS OF THE CALCULATIONS

3.1. Hydrodynamical evolution of the cSNR

Figure 1 shows runs of leading and reverse shocks velocities and radii for 15 M_\odot supernova remnant. The leading shock has initial speed $\sim 4200\ km\ s^{-1}$. Strong radiative cooling in the swept-up CSM matter induces a sudden drop in the post-shock thermal pressure and a noticeable deceleration of the leading shock velocity which falls down from $\sim 3000\ km\ s^{-1}$ to $\sim 2000\ km\ s^{-1}$ during a short transition phase. The process is followed by the condensation of the swept-up interstellar gas into a thin dense shell. The shell density exceeds the shocked ejecta density by about four orders of magnitude. Therefore the CD adjusts the leading shock position and

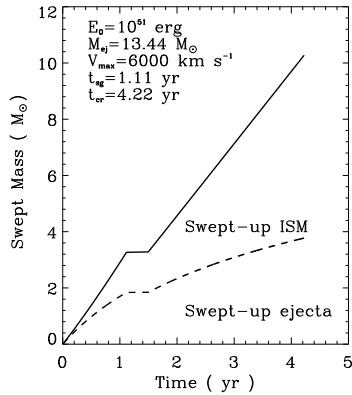


Fig. 2. Swept-up mass evolution.

later on follows its expansion. Radiative phase starts at $t_{sg} \sim 1.2$ yr after explosion and is well identified as breaks of the solid lines at velocity curve.

The reverse shock is substantially slower. It remains adiabatic for a much longer time because of the smaller post-shock density and thus less effective cooling. Shock waves heat both the swept-up circumstellar material and the shocked ejecta to high temperatures $\sim 10^8$ K. However the temperature of the shocked interstellar material suddenly drops when cooling sets in and later on is supported at 10^4 K level by the ionizing photons arising from the cooling shocked gas.

Figure 2 shows the swept-up mass time evolution. The interstellar mass accumulated in the outer shell grows almost linearly with time and at the end of the calculations reaches around $10 M_{\odot}$. During this time the reverse shock processes only $\sim 4 M_{\odot}$ of the ejecta which is spread inside a relatively thick inner shell. The flat parts of the curves in Figure 2 come from our simplified description of the swept-up interstellar mass condensation when catastrophic radiative cooling sets in.

3.2. Chemical evolution of the cSNR

Using the shell thickness and temperature given in the previous section we calculate the characteristic diffusion time t_d one needs to mix the ejected metals with the swept-up CSM. At the beginning of the calculations the characteristic diffusion time grows with time due to the growth of the shell thickness. However when radiative cooling sets in it drops about four orders of magnitude because of the sudden decrease of the outer shell thickness. This leads to an effective and rapid mixing of the ejected metals with the swept-up interstellar matter and defines the fast chemical evolution of the remnant. Initial

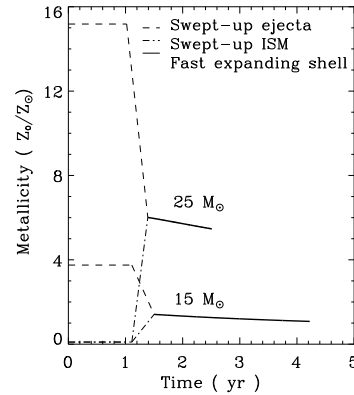


Fig. 3. The cSNR metallicity as function of time if oxygen is used as a tracer.

metallicities of the swept-up interstellar medium and the ejecta and the resultant metallicity of the cSNR outer shell are shown in Figure 3.

4. CONCLUSIONS

The calculations show that effective metal diffusion occurs at early cSNR evolution, soon after a dense shell formation. The resultant shell metallicity was found to be within the range

$1.0 \leq Z/Z_{\odot} \leq 6.0$ if oxygen is used as a tracer and $0.65 \leq Z/Z_{\odot} \leq 1.3$ if iron is used as a tracer of the gas metallicity. This is in a remarkably good coincidence with the observed QSO metal abundances. We speculate therefore that the observed QSO metallicities could be related to SN explosions immersed in a high density CSM.

The authors feel honoured to have attended this meeting and acknowledge support from CONACYT grant 36132-E.

REFERENCES

- Ferland, G. J., Baldwin, J. A., Korista, K. T., Hamann, F., Carswell, R. F., Phillips, M., Wilkes, B., Williams, R. E., 1996, ApJ, 461, 683
- Franco, J., Tenorio-Tagle, G., Bodenheimer, P., R'ozyczka, M., 1991, PASP, 103, 803
- Hamann, F., & Ferland, G. J., 1993, ApJ, 418, 11
- Hamann, F., & Ferland, G. J., 1999, ARA&A, 37, 487
- Oey, S., astro-ph/0211344
- Rodríguez-González, A., MSc Thesis, INAOE, 2002
- Roy, J.-R., Kunth, D., 1995, A&A, 294, 432
- Silk, J. & Rees, M. J., 1998, A&A, 331, L1
- Tenorio-Tagle, G., 1996, Aj, 111, 1641
- Terlevich, R. J., Tenorio-Tagle, G., Franco, J., Melnick, J., 1992, MNRAS, 255, 713
- Woosley, S. E., 1978, ApJ, 225, 1021
- Woosley, S. E., Pinto, P.A. & Ensmann, L., 1988, ApJ, 324, 466